Journal of Medicinal Chemistry

Article

pubs.acs.org/jmc

Methyl Substitution of a Rexinoid Agonist Improves Potency and Reveals Site of Lipid Toxicity

Venkatram R. Atigadda,[†] Gang Xia,[†] Anil Desphande,[†] LeeAnn J. Boerma,[‡] Susan Lobo-Ruppert,[§] Clinton J. Grubbs,[§] Craig D. Smith,[∥] Wayne J. Brouillette,*[,†] and Donald D. Muccio*[,†]

Departments of [†]Chemistry, [‡]Biochemistry and Molecular Genetics, [§]Medicine, and [∥]Vision Sciences, University of Alabama at Birmingham, Birmingham, Alabama 35294, United States

Supporting Information

ABSTRACT: (2*E*,4*E*,6*Z*,8*E*)-8-(3′,4′-Dihydro-1′(2′*H*)-naphthalen-1′-ylidene)-3,7-dimethyl-2,4,6-octatrienoic acid, 9cUAB30, is a selective rexinoid that displays substantial chemopreventive capacity with little toxicity. 4-Methyl-UAB30, an analogue of 9cUAB30, is a potent RXR agonist but caused increased lipid biosynthesis unlike 9cUAB30. To evaluate how methyl substitution influenced potency and lipid biosynthesis, we synthesized four 9cUAB30 homologues with methyl substitutions at the 5-, 6-, 7-, or 8-position of the tetralone ring. The syntheses and biological evaluations of these new analogues are reported here along with the X-ray crystal structures of each homologue bound to the ligand binding domain of hRXRα. We demonstrate that each homologue of 9cUAB30 is a more potent agonist, but only the 7-methyl-9cUAB30 caused severe hyperlipidemia in rats. On the basis of the X-ray crystal structures of these new rexinoids and bexarotene (Targretin) bound to hRXRα-LBD, we reveal that each rexinoid, which induced hyperlipidemia, had methyl groups that interacted with helix 7 residues of the LBD.

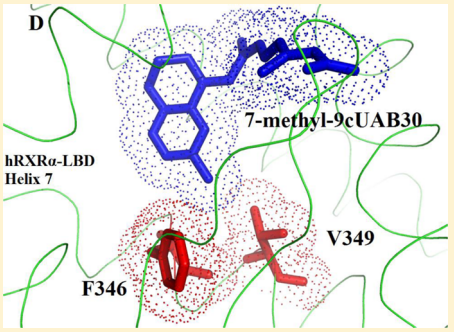

1. INTRODUCTION

Bexarotene (Targretin) is a rexinoid that selectively activates signaling of retinoid X receptors (RXRs) over signaling through retinoic acid receptors (RARs). Bexarotene is the first clinically approved rexinoid, and it is used to treat refractory cutaneous T-cell lymphoma (CTCL).[1] Human phase 1 trials reveal that bexarotene is better tolerated than the RAR agonist, all-*trans*-retinoic acid (ATRA), and the RAR and RXR pan-agonist, 9-*cis*-retinoic acid (9cRA).[2,3] The dose-limiting toxicity of oral bexarotene treatment is hyperlipidemia (both elevated serum triglycerides (TGs) and serum total cholesterol). CTCL patients treated with bexarotene often need to be administered lipid-lowering drugs to control side effects, and if still unmanaged, these patients are removed from bexarotene treatment until lipid levels return to normal ranges.

9cUAB30 is a rexinoid containing a tetralone ring rather than the tetramethyltetrahydronapthelene ring of bexarotene or the trimethylcyclohexenyl ring of 9cRA (Figure 1).[4,5] 9cUAB30, bexarotene, and 9cRA each reduce proliferation, enhance apoptosis in mammary tumors, and efficiently prevent mammary cancers in rodent models.[6] We reported 9cRA, 9cUAB30, and bexarotene each bind to hRXRα-LBD in an L-shaped geometry, and binding of these agonists causes a nearly identical set of conformational changes on the ligand binding domain of human RXRα (hRXRα-LBD) to recruit a coactivator peptide to the surface of the domain.[7,8] There were small differences in these structures localized to the ligand binding pocket. Both 9cRA and bexarotene occupy more volume in this pocket, and each interacts with helices 3 and 7 more than 9cUAB30. These conformational changes and interactions were also present in the 9cUAB30 homologue with a methyl group at the 4-position of the tetralone ring.[9] This homologue of 9cUAB30, 4-methyl-9cUAB30, is more potent than 9cUAB30, but it enhances lipid biosynthesis to an extent exhibited by bexarotene rather than its parent compound. When the gene arrays were analyzed from rat livers obtained from treatment of bexarotene, 4-methyl-9cUAB30, and 9cUAB30, both bexarotene and 4-methyl-9cUAB30 induce signaling through the RXR:LXR heterodimers and the levels of mRNA of key enzymes involved in lipogenesis increase.[10] In contrast, the levels of these key lipogenic liver enzymes of 9cUAB30 treated rats are nearly identical to those from untreated rats, suggesting that this rexinoid is not an agonist in liver tissues (tissue selective).

As mentioned earlier, most of the potent rexinoids including bexarotene and 9cRA are associated with severe hyperlipidemia, which limits their clinical utility for chronic administration. So far it is not clear what structural features of the rexinoids contribute to the increase in lipids. Do the potent rexinoids associated with hyperlipidemia interact differently with the RXR protein than rexinoids which do not induce hyperlipidemia? Our laboratory is engaged in the rational design of rexinoids with significant potency for preventing cancer in the healthy population. Toward this end, we focus in this study on understanding the structural features that contribute to and

Received: March 26, 2014
Published: May 6, 2014

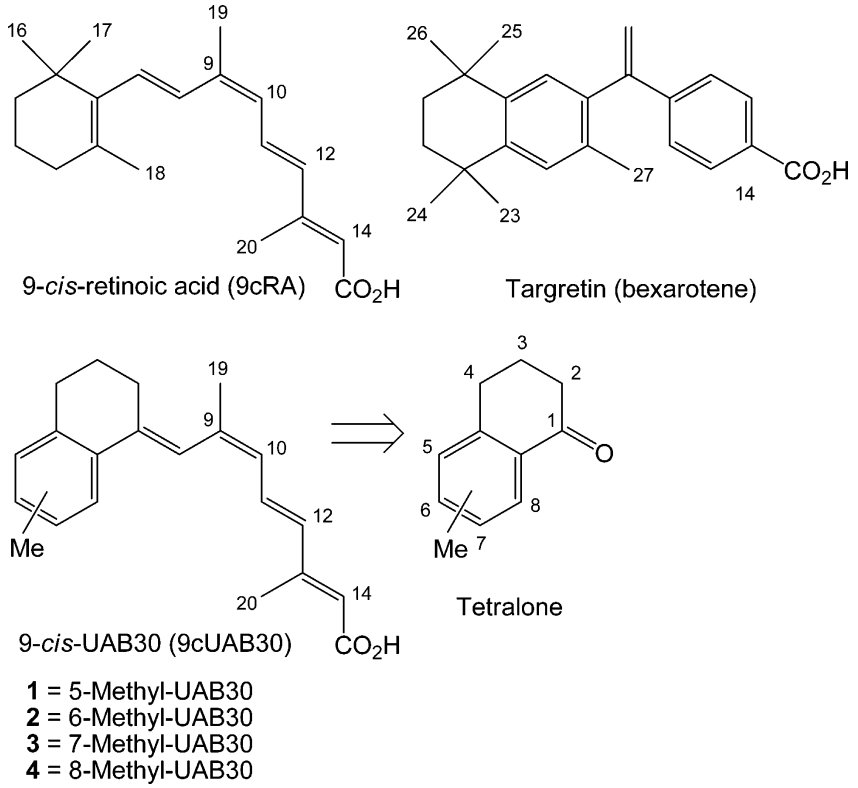

Figure 1. Structures of 9-*cis*-retinoic acid, bexarotene (Targretin), 9-*cis*-UAB30, and four methyl homologues of 9-*cis*-UAB30 (**1**–**4**). The position of the methyl group substitution on 9-*cis*-UAB30 uses the tetralone ring numbering scheme.

Scheme 1. Synthesis of Four 9cUAB30 Homologs with Methyl Substitutions at the 5-, 6-, 7-, or 8-Position of the Tetralone Ring

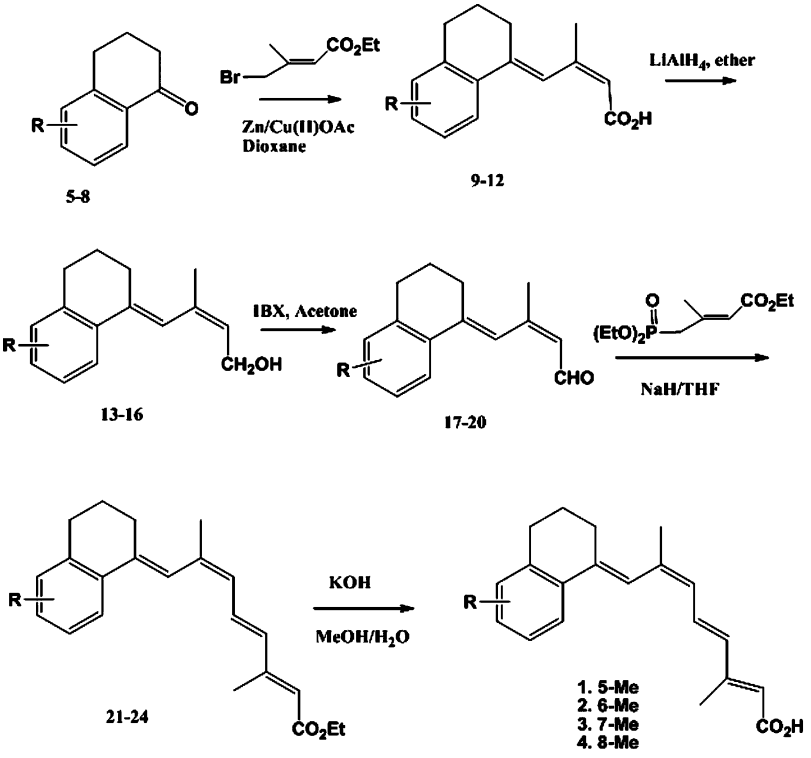

enhance the potency of our parent rexinoid, 9cUAB30, from those structural features that induce hyperlipidemia. Molecular modeling of rexinoids bound to the ligand binding domain of RXR is a common and useful approach in rexinoid design. But we were surprised to find that our low-energy docked structure of 4-methyl-9cUAB30 in the retinoid binding site was quite different from what was found from the actual crystal structures we reported recently.[9] Thus, in this study we synthesized a

dx.doi.org/10.1021/jm5004792 | J. Med. Chem. 2014, 57, 5370−5380

Table 1. Summary of Biological Data for 9cRA, 9cUAB30, and Its Analogues 1−4

retinoid treatment	RXRα binding, K_d (nM)	RXRα activation, EC_{50} (nM)	KLF4 inhibition, EC_{50} (nM)	serum triglyceride, increase (%)	proliferation index, decrease (%)
9cRA	14 ± 3	120 ± 30	110 ± 13	326[a]	56[a]
9cUAB30	33 ± 5	820 ± 70	400 ± 90	63[a]	65[a]
1	18 ± 3	720 ± 20	440 ± 150	31	80
2	15 ± 2	100 ± 30	110 ± 50	51	79
3	8 ± 2	160 ± 10	>1000	642	82
4	10 ± 1	620 ± 50	880	59	29
(*R*)-4-Me-9cUAB30	25 ± 5[b]	120 ± 5[b]	19 ± 4[b]	420[b]	16[b]
bexarotene	26 ± 3[b]	40 ± 6[b]	ND[b]	456[b]	56[b]

[a]Data reported in Grubbs et al.[6] for 150 mg/kg diet for 9cRA and 200 mg/kg diet for 9cUAB30. [b]Data reported in Deshpande et al.[9] for 150 mg/kg diet for bexarotene and 200 mg/kg diet for (*R*)-4-methyl-9cUAB30.

Table 2. Summary of ITC Measurements of GRIP-1 to hRXRα-LBD:UAB Rexinoid Complexes

rexinoid (37 °C)	K_d (μM)	ΔH (kcal/mol)	$-T\Delta S$ (kcal/mol)	ΔG (kcal/mol)	*n*
9cRA	1.56 ± 0.09	−12.3 ± 0.12	4.1	−8.2	0.98
9cUAB30	1.88 ± 0.12	−13.2 ± 0.16	5.1	−8.1	0.96
bexarotene	1.89 ± 0.13	−13.0 ± 0.18	4.9	−8.1	0.96
1	2.24 ± 0.14	−12.6 ± 0.17	4.7	−8.0	0.99
2	1.75 ± 0.08	−13.4 ± 0.11	5.2	−8.2	0.96
3	1.86 ± 0.09	−13.4 ± 0.13	5.2	−8.2	0.96
4	2.33 ± 0.18	−13.0 ± 0.22	5.0	−8.0	0.95
4-Me-9cUAB30	1.55 ± 0.06	−12.6 ± 0.11	4.3	−8.2	0.97

series of methylated analogues of 9cUAB30 and obtained crystal structures for each member of the series. These new analogues (**1**−**4**) possess a single methyl group at the 5-, 6-, 7-, or 8-position of the tetralone ring, which probes the space surrounding the tetralone of 9cUAB30 in a systematic manner (Figure 1). When we compare the structures of methylated 9cUAB30 homologues that induce hyperlipidemia to those we published for bexarotene, we find that rexinoids that significantly induce hyperlipidemia contain one or more methyl groups that interact with the side chains of amino acid residues (F346 and V349) on helix 7 of the LBD of RXR.

2. RESULTS AND DISCUSSION

2.1. Chemistry. Scheme 1 summarizes the methods employed to prepare the new retinoids **1**−**4**. The α-tetralones with methyl substituents (**5**−**8**) were synthesized using previously reported methods.[11−13] The synthesis of retinoids **1**−**4** began with a Reformatsky reaction between methyl substituted α-tetralones **5**−**8** and ethyl 4-bromo-3-methyl-2-butenoate in 1,4-dioxane to provide the 9*Z*-acids **9**−**12** in 60−86% yield. The carboxyl groups in compounds **9**−**12** were then reduced in the presence of $LiAlH_4$ to produce the desired 9*Z*-alcohols **13**−**16** in quantitative yield. The alcohol functional groups in compounds **13**−**16** were next oxidized using IBX to provide the desired 9*Z*-aldehydes **17**−**20** containing minor amounts of all *E*-aldehyde (5−7%). Pure 9*Z*-isomers (**17**−**20**) were isolated in 68−80% yields following column chromatography. Olefination of aldehydes **17**−**20** in the presence of triethyl phosphonosenecioate under Horner−Emmons conditions provided the esters **21**−**25** as an 85:15 mixture of the 9*Z*-isomer to the 9*Z*,13*Z*-isomer. The isomers were readily separated by flash silica column chromatography, and the desired 9*Z*-isomers were obtained in 70−85%. Subsequent hydrolysis of the 9*Z*-esters **21**−**25** under basic conditions provided the final compounds **1**−**4** in 70−85% yields after recrystallization.

2.2. Binding and Transactivation of RXR. 9cRA is a potent pan-agonist for both RARs and RXRs.[14] By use of fluorescence quenching, the 9cRA:hRXRα-LBD homodimer complex had a dissociation constant (K_d) of 14 nM (Table 1).[7] This was consistent with a previously reported result.[15] By use of this method, the K_d for the 9cUAB30:hRXRα-LBD homodimer complex was determined to be 33 ± 5 nM, which was about 2-fold weaker than 9cRA binding. These fluorescence titrations were also performed for the compounds **1**−**4**. Each methyl analogue quenched more than 90% of the fluorescence signal at 337 nm when the ratio of the protein to the rexinoids reached 1:1. The fluorescence quenching data were fit to a single-site binding model, and the K_d values (Table 1) indicated that each methyl analogue of 9cUAB30 bound to the hRXRα-LBD with similar magnitude as 9cRA. Rexinoids **1**−**4** had a 2- to 4-fold stronger binding affinity to hRXRα-LBD than 9cUAB30.

Previous studies have shown that 9cUAB30 is a RXR-selective agonist in two cell lines while 9cRA is a potent pan-agonist.[5,16] In RK3E cells, the EC_{50} value for 9cUAB30 activating RXRα transcription was about 6-fold weaker than for 9cRA activation and it was a full agonist (Table 1). Using 9cRA as a positive control, 9cUAB30 did not activate RARα-mediated transcription at a high concentration (<1% at 10^{-6} M). Using these receptor reporter assays in RK3E cells, we evaluated the capability of methyl-substituted 9cUAB30 analogues (**1**−**4**) for activating RXRα. The EC_{50} values for RXRα activation by **1** and **4** were similar to 9cUAB30; however, the EC_{50} values of **2** and **4** were much lower than that for 9cUAB30 and similar to that found for 9cRA (Table 1). When RARα activation was examined, rexinoids **1**−**3** did not activate transcription relative to controls (less than 1%); however, rexinoid **4** induced 20% activation of RAR-mediated transcription only at the highest dose tested (10^{-6} M).

We used isothermal titration calorimetry (ITC) to measure GRIP-1 binding to hRXRα-LBD homodimers containing 9cUAB30 or its methylated analogues. All measurements

dx.doi.org/10.1021/jm5004792 | J. Med. Chem. 2014, 57, 5370−5380

were performed at 37 °C. When 9cRA, 9cUAB30, or bexarotene was bound to hRXRα-LBD homodimers, GRIP-1 occupied both coactivator binding sites on the monomers (stoichiometry nearly 1:1 for GRIP-1/hRXRα-LBD monomer subunit). For rexinoids **1**−**4**, the stoichiometries for GRIP-1 binding were all near 1:1. This indicates that these homologues of 9cUAB30 can recruit coactivators to both binding sites on the surface of the LBD, and it is consistent with their agonist properties. The free energy of GRIP-1 binding to the hRXRα-LBD complexes containing rexinoids **1**−**4** was similar in magnitude (−8.1 ± 0.1 kcal/mol). The negative free energy change for GRIP-1 binding was driven strongly by a large negative enthalpy change (−13.0 ± 0.4 kcal/mol) regardless of which homologue of 9cUAB30 was present in the LBP. Likewise, binding was opposed by entropy even though the coactivator peptide contains the ILxxLL hydrophobic motif (Table 2). This thermodynamic signature for GRIP-1 binding to homodimers was very similar for GRIP-1 binding to homodimers containing two other rexinoids (9cUAB30 or bexarotene) or the pan-agonist 9cRA in its LBP (Table 2).[7]

2.3. Inhibition of Oncogenic Transformation. Previously we showed that the pan-agonist 9cRA and two RXR-selective agonists, 9cUAB30 and bexarotene, inhibited transformation of rat kidney epithelial (RK3E) cells infected with the oncogene KLF4.[16] 9cUAB30 was 3-fold less effective than 9cRA in this assay (Table 1). We demonstrated that 4-methyl-9cUAB30 had equal potency to 9cRA in blocking oncogenesis. Most of the potency of this racemic rexinoid was present in the (*S*)-enantiomer.[9] Here, the potencies of the 9cUAB30 methyl analogues **1**−**4** in blocking transformation of oncogenes were compared to the activity of 9cUAB30. Relative to DMSO, **2** was the most potent methyl homologue for the inhibition of KLF4-ER mediated transformation. Homologue **1** had potency similar to 9cUAB30, while **4** was 2-fold less active than the parent rexinoid (Table 1). The inhibition of transformation correlated well with reduction of squamous cell carcinoma in the skin in transgenic mice models.[16] These studies indicate that **2** has the most promising potential for preventing squamous cell carcinoma of the skin.

2.4. In Vivo Triglyceride Levels and Inhibition of Proliferation of Rat Mammary Cancers. The elevation of serum triglyceride (TG) is a dose limiting toxicity of many rexinoids like bexarotene.[3] In contrast the tissue-selective 9cUAB30 did not increase serum TG in chronic administration in preclinical evaluation in rodents and dogs or as a single dose in humans.[17,18] In order to study if methyl homologues of 9cUAB30 had a similar effect, we measured serum TG in rats (216 days of age) fed a diet of rexinoids **1**−**4** containing 200 mg/kg diet. As displayed in Table 1, rexinoids **1**, **2**, and **4** increased serum TG only slightly (30−60%), but rexinoid **3** raised TG levels by 642% over controls. There was a dose response to the TG increase; rats fed a diet containing only 100 mg rexinoid/kg diet increased serum TG by 206%. No dose response was observed for rexinoids **1**, **2**, **4** or the parent rexinoid 9cUAB30. There was no change in the body weights of the rats for all treated groups in comparison to the controls. Liver weights normalized to body weight also showed no variation from the control rats.

Proliferation of estrogen receptor-positive mammary cancers is decreased using estrogen receptor antagonists or agents that block estrogen biosynthesis. Potent rexinoid agonists also decrease proliferation as we demonstrated for bexarotene, 9cUAB30, and 4-methyl-UAB30.[7−9] The decrease in BRDU proliferation index correlates well with their capacity to prevent estrogen receptor-positive mammary cancers.[6] We evaluated each of these analogues **1**−**4** in antiproliferative assays using rats with established mammary cancers induced by the chemical carcinogen *N*-methylnitrosourea. As displayed in Table 1, for rexinoids **1**−**3** the proliferation index decreased by 79−82% when rats containing existing mammary cancers were fed for 7 days a diet containing 200 mg/kg **1**, **2**, or **3**. The decrease in proliferation index was only 29% in rat tumors treated with oral dosing of **4** (Table 1).

2.5. Crystal Structures of hRXRα-LBD Homodimers Bound with Methyl Homologues. Previously we determined the X-ray crystal structures of hRXRα-LBD homodimers bound to the pan-agonist 9cRA with the coactivator peptide GRIP-1 (^{686}KHKILHRLLQDSS^{698}).[7] We also used this coactivator peptide when we compared the structures of bexarotene to 9cUAB30 bound to hRXRα-LBD homodimer[8] or when we compared the structures of (*R*)-4-methyl-9cUAB30 and (*S*)-4-methyl-9cUAB30 to that of 9cUAB30.[9] Here we report four additional crystal structures of hRXRα-LBD homodimers containing rexinoid **1** (PDB code 4PP5), **2** (PDB code 4PP3), **3** (PDB code 4PPJ), or **4** (PDB code 4POH) in the presence of coactivator peptide GRIP-1. Each crystal structure belonged to the $P4_{(3)}2_{(1)}2$ space group, and each unit cell contained two monomers with GRIP-1 bound to each monomer. The summary of the X-ray crystallography and refinement statistics for the structures are provided in the Supporting Information.

The 3D fold of the hRXRα-LBD homodimer was nearly identical regardless which 9cUAB30 homologue was bound. The backbone atoms of each structure were overlaid with the structure of hRXRα-LBD bound to 9cUAB30 and GRIP-1 complex (4K4J). The rmsd values for this overlay of 229 backbone residues were 0.130, 0.139, 0.105, and 0.128 for homodimers bound to **1**, **2**, **3**, and **4**, respectively (Figure 2).

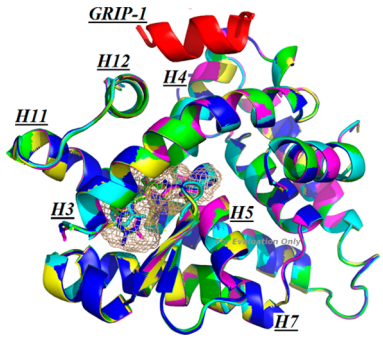

Figure 2. Overlay of X-ray crystal structures of hRXRα-LBD bound to 9cUAB30 (green), **1** (yellow), **2** (blue), **3** (magenta), and **4** (cyan). The coactivator peptide GRIP-1 is displayed in red, and the ligand binding pocket of hRXRα-LBD is highlighted in brown-gray mesh.

We established that four conformational changes occur in the layer between the rexinoid binding site and the coactivator binding site.[7,8] Each of these conformational changes was present in the structures containing the methyl homologues studied here. These allow helix 12 of the hRXRα-LBD to form the coactivator binding site. Together with helices 3 and 4 residues, the ILxxLL motif of GRIP-1 bound to the hydrophobic pocket on the surface of the receptor and GRIP-1 was held by charge clamps. These interactions were identical for the structures reported here and those reported previously.[7] The

dx.doi.org/10.1021/jm5004792 | J. Med. Chem. 2014, 57, 5370−5380

only exception occurred when rexinoid **2** was bound. In this structure, the side chain of E456 (helix 12) extended completely into the solvent and the charge clamp was not formed with H687 on GRIP-1.

2.6. Ligand Binding Pocket of hRXRα-LBD Bound to Methyl Homologues. The ligand binding pocket is defined by residues from four helices (helices 3, 5, 7, and 11) with a few residues from the β sheet. The ligand binding pocket is buried near the center of the ligand binding domain and away from the coactivator binding site. Rexinoids **1**, **2**, **3**, and **4** adopted an L-shaped conformation inside the ligand binding pocket (LBP) of hRXRα-LBD, and these conformations were similar to the twisted conformations of 9cRA, 9cUAB30, 4-methyl-UAB30 enantiomers or bexarotene in the LBP.[7,8] Rexinoids **1**–**4** contain a twisted C8–C9 torsional angle, and these rexinoids also adopt an L-shape in the LBP similar to 9cUAB30 (Figure 3A and Figure 3B). The C8–C9 dihedral angles of **1**–**3** were

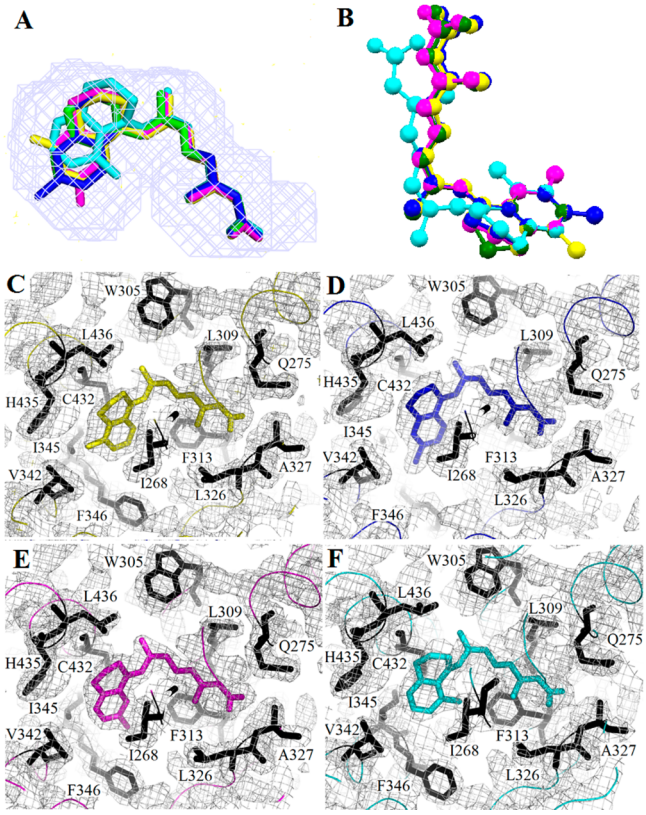

Figure 3. (A) Overlay of UAB rexinoids in the ligand binding pocket of hRXRα-LBD: 9cUAB30 (green), **1** (yellow), **2** (blue), **3** (magenta), and **4** (cyan). (B) Side view of this overlay showing the common L-shaped twist in the rexinoid structure and the tetralone ring pucker. (C–F). Electron density maps ($2F_o - F_c$) for the ligand binding pocket containing **1** (C), **2** (D), **3** (E), and **4** (F).

121.6°, 123.5°, 124.7°, respectively. These torsional angles were close to the torsional angle found when 9cUAB30 occupied the LBP (121.4°). The twisted conformation of the rexinoids reduced steric effects between the C2 and C3 methylene groups of the tetralone ring and the methyl group at C9 (C19). The C8–C9 dihedral angle on rexinoid **4** (102°) was noticeably smaller than the angle measured for 9cUAB30 and the other methyl homologues. This decrease in dihedral angle was due to interactions between the methyl group on the 8-position of the tetralone ring and H8 of the tetraene chain. The observed orientation of the tetralone ring in compounds **1**–**4** and 9cUAB30 were in distinct contrast to those of (*S*)-4-methyl-9cUAB30 (C8–C9 = −56.6°) and (*R*)-4-methyl-9cUAB30 (C8–C9 = −64.4°), where the tetralone ring was flipped by nearly 180° in the ligand binding pocket relative to 9cUAB30 and the other methyl homologues, **1**–**4**.

In the bound structure of 9cUAB30, the cyclohexenyl ring adopted a half-chair conformation with the C3 methylene of the tetralone ring pointed to the same side as C19, and the C2 methylene was on the opposite side. The dihedral angle of C2–C3 in 9cUAB30 was 51.9°. This orientation reduced the steric effect between the C19 methyl group on C9 and the methylene group on C2 on the tetralone ring. The conformations of the tetralone ring for **1**–**4** were different from those of 9cUAB30. Both the C2 and C3 atoms in rexinoids **1**–**4** were in a twisted envelope conformation (Figure 3B). The C2–C3 dihedral angles for rexinoids **1**–**4** were −43.0°, −41.8°, −44.3°, and −9.8°, respectively. C2 and C3 were on the same side of the tetralone ring plane and pointed in the opposite direction of C19 in order to avoid any unfavorable steric interactions with C19.

2.7. Ligand Protein Contacts between Rexinoids and hRXRα-LBD. In the crystal structures of hRXRα-LBD:UAB rexinoid/GRIP-1 complexes, 9cUAB30 and its methyl analogues were completely buried in the LBP of hRXRα-LBD. Rexinoid **1** had a similar orientation in the LBP as 9cUAB30. The methyl group at the 5-position in **1** resulted in 30% more contact area with V342 and I345 on helix 7 than 9cUAB30 (Figure 3C). The carboxylate group in rexinoid **1** was also closer to the β sheet than 9cUAB30. For **2**, the methyl group at the 6-position of the tetralone ring made more contacts with V342 and F346 on helix 7 than observed for 9cUAB30. The phenyl ring of F346 rotated by 37° (along the C_β) to avoid unfavorable steric interaction with the methyl group on C6 (Figure 3D). Rexinoid **3** contains a methyl group at the 7-position on the tetralone ring. This methyl group interacted with F346 and V349 (Figure 3E). The position of rexinoid **4** in the LBP was much different from those of rexinoids **1**–**3** and the parent compound 9cUAB30. Rexinoid **4** was shifted by 1.2 Å toward helices 3 and 5 (Figure 3F). This movement led to an increased surface area contact with helix 3 (10%) and helix 5 (17%) and a decreased surface area contact with helix 7 (19%) relative to 9cUAB30. The methyl group at the 8 position in **4** interacted strongly with I268 of helix 3, a residue with which 9cUAB30 had very little contact.

2.8. Comparison of Structural Results and Biological Activities. In our previous publications, we examined the structures of 9cUAB30, 4-methyl-9cUAB30 enantiomers, bexarotene, and 9cRA bound to hRXRα-LBD homodimers with GRIP-1.[7–9] The crystal structure of bexarotene revealed that the C23/C24 methyl groups pointed toward helix 7 (Figure 4A). These methyl groups were tightly positioned between V349 and F346 (3.7–4.6 Å), and they made strong van der Waals contacts to each of these residues. In the crystal structure of 9cUAB30 bound to this protein domain (Figure 4B), these interactions were missing. Only minor van der Waals interactions occurred between the methylene groups of the tetralone and F346/V349. In the crystal structures of (*R*)- and (*S*)-4-methyl-9cUAB30 bound to the RXR LBD, we found that the methyl group at the 4-position on the tetralone of each enantiomer occupied a similar space in the LBP as the C23/C24 methyl groups of bexarotene (Figure 4C). Using the bound structure of 9cUAB30 as a guide, we expected the 4-

dx.doi.org/10.1021/jm5004792 | J. Med. Chem. 2014, 57, 5370–5380

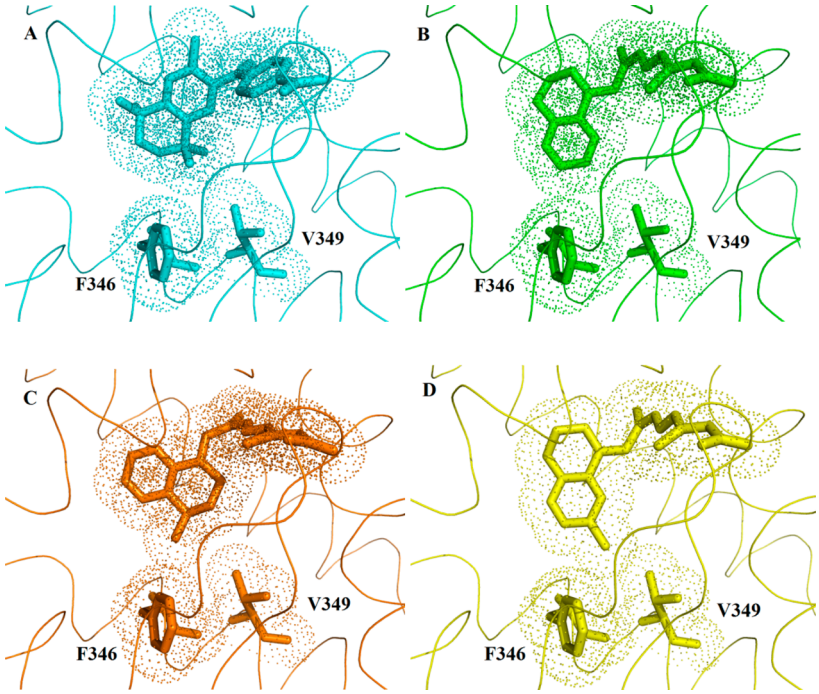

Figure 4. Interactions between the rexinoid rings with helix 7 residues, F346 and V347, with van der Waals surfaces of rexinoid and protein residues shown as dots: bexarotene (Targretin) (A), 9cUAB30 (B), 4-methyl-UAB30 (C), and 7-methyl-UAB30, **3** (D).

methyl group to be oriented toward helix 11 residues. However, the conformation of the tetralone ring of 4-methyl-9cUAB30 enantiomers changed because of a nearly 180° rotation around the C8−C9 bond. The conformational change in the backbone of the polyene chain reoriented the tetralone to optimize van der Waals interactions between the methyl group at the 4-position of the tetralone and helix 7 residues (3.5−4.4 Å). It is well-established that bexarotene and 4-methyl-9cUAB30 enantiomers raise serum triglycerides significantly when fed to rodents, whereas 9cUAB30 displays minimal effect on triglyceride levels.[9] In a recent publication, genomic studies of liver tissues from animals treated with bexarotene and racemic 4-methyl-UAB30 demonstrated that the signaling pathways for lipogenesis were enhanced by rexinoid activation of RXR−LXR heterodimers.[10] In contrast to these rexinoids, liver tissues from 9cUAB30-treated rats did not affect these lipogenic pathways.[10]

Prior studies suggest that rexinoids with structural features that interact with helix 7 residues may cause enhanced lipogenesis. To test this hypothesis, the structures of several 9cUAB30 homologues were analyzed bound to RXR LBD containing the GRIP-1 coactivator peptide. These homologues position methyl groups systematically around the tetralone ring. Homologue **3** is a potent agonist that contains a methyl group at the 7-position of the tetralone ring (Table 1). The crystal structure of **3** bound to this protein domain revealed an L-shaped conformation that was similar to 9cUAB30 (Figure 3), which allowed for the methyl group on position 7 to be directed toward helix 7 residues F346/V349 (Figure 4D). In a similar fashion to bexarotene and 4-methyl-UAB30, the 7-methyl group of **3** made strong contact with V349 (3.88 Å) and F346 (3.70 Å). The serum TG levels of rodents dosed with **3** at 200 mg/kg diet for 7 days were increased by over 600% in a dose-dependent manner, further reinforcing the argument that the strong lipophilic interactions between the rexinoid and these helix 7 residues of RXR lead to signaling that enhances lipogenesis. Methyl homologues **1**, **2**, and **4** did not significantly induce lipogenesis, even though they were potent RXR agonists (Table 1). The methyl group at the 6-position of the tetralone ring of homologue **2** was pointed toward the N-terminal end of helix 7, but it made no direct van der Waals contact with F346/V349. A small conformational change occurred in this crystal structure, and the phenyl ring of F346 rotated away from the rexinoid by about 34° (data not shown). For methyl homologues **1** and **4**, which have methyl groups at the 5- and 8-positions of the tetralone ring, there were essentially no contacts with helix 7 residues (data not shown). Both homologues **1** and **4** bound strongly and activated RXR, without significantly affecting serum triglyceride levels. It should be noted that homologue **4** was shifted in the LBP toward helices 5 and 11 to prevent the steric crowding between the methyl group and I268 on helix 3.

3. CONCLUSIONS

In this study we demonstrate that methyl substitution of 9cUAB30 improved the potency relative to the parent RXRα agonist, 9cUAB30, by nearly 10-fold. This is consistent with the increased potency we observed for 4-methyl-9cUAB30 enantiomers and how methyl substitution often affects the potency of other drugs.[9,19] Rexinoid **2** displays efficacy in all biological evaluations of cancer prevention and therapy while not influencing signaling that elevates serum triglyceride levels. These results warrant further evaluation of rexinoid **2** for chemoprevention. This study further improved our understanding of the rexinoid−protein interactions and more importantly shed light on the interactions between rexinoid and helix 7 residues that may contribute to lipogenesis. Taken together, subtle changes in lipophilic interactions in this region of the rexinoid binding pocket may account for the undesired lipogenesis by enhancing signaling of RXR−LXR heterodimers, which control many lipogenic genes.

dx.doi.org/10.1021/jm5004792 | J. Med. Chem. 2014, 57, 5370−5380

4. EXPERIMENTAL SECTION

^{1}H and ^{13}C NMR spectra were recorded on Bruker ARX 300 and DRX 400 spectrometers. IR spectra were recorded using a ABB Bomem FTIR spectrometer. UV−vis spectra were recorded on a Varian (Carry 100 Conc) spectrophotometer in methanol (Aldrich, spectrograde). Mass spectra were taken on a Hewlett-Packard 1100 LC−MS instrument and ionized by using electrospray ionization (ESI). Melting points were recorded on an Electrothermal melting point apparatus and are uncorrected. All reactions, unless otherwise mentioned, were monitored by thin layer chromatography (TLC) on 0.25 mm silica gel plates (60F-254, E. Merck or Silicycle). Flash chromatography was performed using Silicycle silica gel (40−63 μm). Reactions and purifications were conducted with nitrogen-saturated solvents and under subdued lighting. Ethyl 4-bromo-3-methylbut-2-enoate was prepared by the reaction of ethyl 3,3-dimethylacrylate with *N*-bromosuccinimide.[20] Triethyl phosphonosenecioate was prepared via the Arbusov reaction.[21] Purity of the all the compounds were determined to be ≥95% which was determined by combustion analysis performed by Atlantic Microlabs, Inc. (Norcross, GA).

(2*Z*,4*E*)-4-[5′-Methyl-3′,4′-dihydro-1′(2′*H*)-naphthalen-1′-ylidene]-3-methyl-2-butenoic Acid (9). A suspension of Zn dust (12.60 g, 192.0 mmol) and copper(II) acetate (1.30 g) in glacial acetic acid (40 mL) was stirred under nitrogen for 1 h in a 250 mL round-bottomed flask. The mixture was diluted with anhydrous ether (50 mL) and vacuum-filtered using a sintered glass funnel under air. The Zn−Cu complex was then washed successively with anhydrous ether (3 × 20 mL) and anhydrous benzene (3 × 20 mL). This complex was dried under vacuum for 1 h at room temperature and transferred to a 250 mL, flame-dried, three-neck flask fitted with a condenser, addition funnel, and nitrogen inlet. Anhydrous dioxane (50 mL) was transferred to the flask, and this suspension was heated to 90 °C in an oil bath. This reaction mixture was then treated dropwise with a solution of 5-methyltetralone (**5**) (8.80 g, 55.0 mmol) and ethyl 4-bromo-3-methylbut-2-enoate (22.8 g, 110 mmol) in dry dioxane (50 mL). Vigorous bubbling was noticed during the addition process, and the reaction mixture was stirred at reflux for 8 h and then cooled to room temperature. Water (50 mL) and 2 N HCl (50 mL) were added. The mixture was diluted with ether (100 mL) and allowed to stir for 10 min. The mixture was filtered, and the acidic layer was separated. The organic layer was washed with water (2 × 50 mL) and then with 1 N NaOH (3 × 40 mL). The combined basic layers were cooled in an ice bath, and the pH of the solution was adjusted to ∼2 with HCl (2 N). The product was extracted into ether (3 × 40 mL), and the combined organic layers were washed with water (40 mL), brine (40 mL), dried (Na_2SO_4), and evaporated under vacuum to give a semisolid that was crystallized from ether/hexanes to obtain pure **9** (9.98 g, 75.0% yield): mp 153−155 °C [ether/hexanes (1:2)]; UV λ_{max} 301 nm (ε = 10 729); IR (KBr) 2938 (−OH), 1669 (C═O), 1607 (C═C) cm^{-1}; MS *m*/*z* 243.45 (MH$^+$); ^{1}H NMR (300 MHz, $CDCl_3$) δ 7.51−7.47 (m, 1H), 7.07 (d, *J* = 4.5 Hz, 2H), 7.02 (s, 1H), 5.79 (s, 1H), 2.69 (t, *J* = 6.6 Hz, 2H), 2.52−2.48 (m, 2H), 2.23 (s, 3H), 2.11 (s, 3H), 1.93−1.84 (m, 2H); ^{13}C NMR (75 MHz, $CDCl_3$) δ 171.73, 156.23, 141.04, 136.50, 136.25, 129.58, 125.86, 123.17, 122.12, 118.08, 28.33, 27.15, 25.99, 23.46, 19.91.

(2*Z*,4*E*)-4-[6′-Methyl-3′,4′-dihydro-1′(2′*H*)-naphthalen-1′-ylidene]-3-methyl-2-butenoic Acid (10). A Zn−Cu complex was generated as described earlier, from Zn dust (11.4 g, 175.0 mmol) and copper(II) acetate (1.15 g) in glacial acetic acid (40 mL). This complex in dry dioxane (50 mL) was treated with a solution of 6-methyltetralone **6** (8.00 g, 50.0 mmol) and ethyl 4-bromo-3-methylbut-2-enoate (20.7 g, 100 mmol) in dry dioxane (50 mL). Following the usual workup provided **10** (8.35 g, 69.0% yield): mp 149−151 °C [ether/hexanes (1:2)]; UV λ_{max} 308 (ε = 13 491); IR (KBr) 2941 (−OH), 1681 (C═O), 1621 (C═C) cm^{-1}; MS *m*/*z* 243.60 (MH$^+$); ^{1}H NMR (300 MHz, $CDCl_3$) δ 7.56 (d, *J* = 8.1 Hz, 1H), 7.16 (s, 1H), 6.97 (d, *J* = 8.2 Hz, 1H), 6.91 (s, 1H), 5.76 (s, 1H), 2.76 (t, *J* = 6.3 Hz, 2H), 2.60−2.55 (m, 2H), 2.30 (s, 3H), 2.13 (s, 3H), 1.86−1.78 (m, 2H); ^{13}C NMR (75 MHz, $CDCl_3$) δ 171.48, 156.19, 140.32, 138.33, 137.85, 133.17, 129.75, 127.37, 125.05, 121.34, 117.93, 30.37, 29.00, 25.96, 23.54, 21.28.

(2*Z*,4*E*)-4-[7′-Methyl-3′,4′-dihydro-1′(2′*H*)-naphthalen-1′-ylidene]-3-methyl-2-butenoic Acid (11). A Zn−Cu complex was generated as described earlier, from Zn dust (12.59 g, 192.0 mmol) and copper(II) acetate (1.30 g) in glacial acetic acid (40 mL). This complex in dry dioxane (50 mL) was treated with a solution of 7-methyltetralone **7** (8.80 g, 55.0 mmol) and ethyl 4-bromo-3-methylbut-2-enoate (22.8 g, 110 mmol) in dry dioxane (50 mL). Following the usual workup provided **11** (10.2 g, 77.0% yield): mp 127−129 °C [ether/hexanes (1:2)]; UV λ_{max} 309 (ε = 11 637); IR (KBr) 2944 (−OH), 1665 (C═O), 1623 (C═C) cm^{-1}; MS *m*/*z* 243.42 (MH$^+$); ^{1}H NMR (300 MHz, $CDCl_3$) δ 7.45 (s, 1H), 7.08 (s, 1H), 6.98 (m, 2H), 5.78 (s, 1H), 2.75 (t, *J* = 6.2 Hz, 2H), 2.56−2.51 (m, 2H), 2.29 (s, 3H), 2.10 (s, 3H), 1.85−1.77 (m, 2H); ^{13}C NMR (75 MHz, $CDCl_3$) δ 171.73, 156.24, 140.08, 135.64, 135.57, 135.37, 129.11, 128.91, 125.41, 121.95, 118.09, 29.93, 28.85, 25.93, 23.63, 21.39.

(2*Z*,4*E*)-4-[8′-Methyl-3′,4′-dihydro-1′(2′*H*)-naphthalen-1′-ylidene]-3-methyl-2-butenoic Acid (12). A Zn−Cu complex was generated as described earlier, from Zn dust (9.15 g, 140.0 mmol) and copper(II) acetate (1.0 g) in glacial acetic acid (30 mL). This complex in dry dioxane (40 mL) was treated with a solution of 8-methyltetralone **8** (6.40 g, 40.0 mmol) and ethyl 4-bromo-3-methylbut-2-enoate (16.6 g, 80.0 mmol) in dry dioxane (40 mL). Following the usual workup provided **12** (6.00 g, 62.0% yield): mp 158−160 °C [ether/hexanes (1:2)]; UV λ_{max} 287 (ε = 16 226); IR (KBr) 2944 (OH), 1676 (C═O), 1654 (C═C) cm^{-1}; MS *m*/*z* 243.45 (MH$^+$); ^{1}H NMR (300 MHz, $CDCl_3$) δ 7.07 (d, *J* = 4.8 Hz, 2H), 6.93 (t, *J* = 4.5 Hz, 1H), 6.52 (s, 1H), 5.78 (s, 1H), 2.59 (t, *J* = 6.2 Hz, 2H), 2.51−2.48 (m, 2H), 2.46 (s, 3H), 2.09 (s, 3H), 1.79−1.70 (m, 2H); ^{13}C NMR (75 MHz, $CDCl_3$) δ 171.62, 155.73, 140.69, 139.24, 138.28, 135.03, 129.47, 127.76, 126.81, 125.14, 118.01, 30.10, 27.96, 26.14, 22.63, 21.44.

(2*Z*,4*E*)-4-[5′-Methyl-3′,4′-dihydro-1′(2′*H*)-naphthalen-1′-ylidene]-3-methyl-2-butenol (13). To a flame-dried two-neck round-bottomed flask fitted with a nitrogen inlet and addition funnel were added acid **9** (7.26 g, 30.0 mmol) and anhydrous ether (100 mL). The flask was cooled to 0 °C in an ice bath, and the reaction mixture was treated with 1 M $LiAlH_4$/ether (39 mL, 39.0 mmol) dropwise. The mixture was stirred for 2 h at 0 °C, cooled to −80 °C in a dry ice/acetone bath, and slowly quenched with methanol (5 mL) followed by 1 N HCl (40 mL). The reaction mixture was allowed to come to room temperature and extracted with ether (3 × 75 mL). The combined ether layers were washed with water (40 mL), brine (40 mL), dried (Na_2SO_4), and concentrated under vacuum to give the alcohol **13**: mp 79−81 °C [ether/hexanes (1:2)]; UV λ_{max} 267.5 (ε = 15 390); IR (KBr) 3307 (−OH), 1656 (C═C), 1624 (C═C) cm^{-1}; MS *m*/*z* 211.51 (MH$^+$ − H_2O); ^{1}H NMR (300 MHz, $CDCl_3$) δ 7.50−7.40 (m, 1H), 7.15−7.03 (m, 2H), 6.32 (s, 1H), 5.55 (t, *J* = 6.6 Hz, 1H), 4.06 (d, *J* = 6.7 Hz, 2H), 2.70 (t, *J* = 6.5 Hz, 2H), 2.32 (m, 2H), 2.23 (s, 3H), 1.91−1.80 (m, 2H), 1.86 (s 3H), 1.40 (brs, 1H); ^{13}C NMR (75 MHz, $CDCl_3$) δ 138.64, 136.74, 136.45, 136.02, 135.95, 129.19, 126.36, 125.72, 122.51, 122.06, 61.08, 27.66, 27.30, 24.25, 23.86, 19.94.

(2*Z*,4*E*)-4-[6′-Methyl-3′,4′-dihydro-1′(2′*H*)-naphthalen-1′-ylidene]-3-methyl-2-butenol (14). This preparation employed the acid **10** (6.05 g, 25.0 mmol) in anhydrous ether (75 mL) and 1 M $LiAlH_4$/ether (32.5 mL, 33.0 mmol). After the workup described above was obtained the alcohol **14** (5.36 g, 94.0% yield) as an oil: UV λ_{max} 268 (ε = 10 465); IR (neat) 3340 (−OH), 1610 (C═C),cm^{-1}; MS *m*/*z* 211.55 (MH$^+$ − H_2O); ^{1}H NMR (400 MHz, $CDCl_3$) δ 7.49 (d, *J* = 8.1 Hz, 1H), 6.98 (d, *J* = 8.1 Hz, 1H), 6.93 (s, 1H), 6.35 (s, 1H), 5.55 (t, *J* = 6.4 Hz, 1H), 4.06 (d, *J* = 6.7 Hz, 2H), 2.80 (t, *J* = 6.3 Hz, 2H), 2.35 (m, 2H), 2.31 (s, 3H), 1.87 (s, 3H), 1.85−1.78 (m, 2H), 1.55 (brs, 1H); ^{13}C NMR (100 MHz, $CDCl_3$) δ 139.52, 139.42, 139.34, 138.56, 134.86, 131.92, 129.11, 128.30, 126.26, 123.23, 63.15, 32.37, 30.27, 26.25, 25.89, 23.22.

(2*Z*,4*E*)-4-[7′-Methyl-3′,4′-dihydro-1′(2′*H*)-naphthalen-1′-ylidene]-3-methyl-2-butenol (15). This preparation employed the acid **11** (8.00 g, 34.0 mmol) in anhydrous ether (100 mL) and 1 M $LiAlH_4$/ether (43 mL, 43.0 mmol). After workup as described earlier

dx.doi.org/10.1021/jm5004792 | *J. Med. Chem.* 2014, 57, 5370−5380

was obtained the alcohol **15** (7.08 g, 94% yield) as an oil: UV λ_{max} 264 (ε = 12 516); IR (neat) 3332 (−OH), 1607 (C═C),cm^{-1}; MS *m*/*z* 211.32 ($MH^+ - H_2O$); ^{1}H NMR (300 MHz, $CDCl_3$) δ 7.41 (s, 1H), 7.00 (m, 2H), 6.36 (s, 1H), 5.55 (t, *J* = 6.6 Hz, 1H), 4.06 (d, *J* = 6.7 Hz, 2H), 2.79 (t, *J* = 6.3 Hz, 2H), 2.35 (m, 2H), 2.32 (s, 3H), 1.86 (s 3H), 1.86−1.76 (m, 2H), 1.57 (brs, 1H); ^{13}C NMR (75 MHz, $CDCl_3$) δ 137.61, 136.41, 135.45, 135.37, 134.67, 129.28, 128.48, 126.38, 124.73, 121.93, 61.05, 29.95, 28.19, 24.17, 23.97, 21.37.

(2*Z*,4*E*)-4-[8′-Methyl-3′,4′-dihydro-1′(2′*H*)-naphthalen-1′-ylidene]-3-methyl-2-butenol (16). This preparation employed the acid **12** (5.56 g, 23.0 mmol) in anhydrous ether (75 mL) and 1 M $LiAlH_4$/ether (30 mL, 30.0 mmol). After the workup described earlier was obtained the alcohol **16** (5.03 g, 96.0% yield) as an oil: IR (neat) 3332 (−OH), 1607 (C═C) cm^{-1}; MS *m*/*z* 229.55 (MH^+); ^{1}H NMR (300 MHz, $CDCl_3$) δ 7.08 (m, 2H), 6.95 (m, 1H), 5.93 (s, 1H), 5.57 (t, *J* = 6.7 Hz, 1H), 4.15 (d, *J* = 6.6 Hz, 2H), 2.62 (t, *J* = 6.4 Hz, 2H), 2.45 (s, 3H), 2.33 (m, 2H), 1.85 (s 3H), 1.80−1.71 (m, 2H), 1.55 (brs, 1H); ^{13}C NMR (75 MHz, $CDCl_3$) δ 140.36, 138.26, 136.88, 136.30, 134.42, 129.32, 128.25, 126.53, 126.50, 125.28, 61.32, 30.18, 27.38, 24.21, 23.03, 21.73.

(2*Z*,4*E*)-4-[5′-Methyl-3′,4′-dihydro-1′(2′*H*)-naphthalen-1′-ylidene]-3-methyl-2-butenal (17). A single-neck round bottomed flask fitted with a reflux condenser was charged with *o*-iodoxybenzoic acid (IBX) (28.0 g, 100 mmol) and acetone (100 mL) and warmed to 50−55 °C in an oil bath. A solution of alcohol **13** (5.70 g, 25.0 mmol) in acetone (25 mL) was added all at once to the reaction mixture. The mixture was then allowed to stir at 50−55 °C for 1.5 h. It should be noted that IBX at temperatures greater than 200 °C has been demonstrated to be explosive. We have not experienced any problematic incidents with IBX used in these reactions. The reaction mixture was cooled to 0 °C in an ice bath, diluted with ether (50 mL), and filtered through a sintered glass funnel. The filtrate (solids retained on the funnel) was washed with ether (2 × 75 mL), and the combined organic layers were concentrated under vacuum to furnish the crude product **17** (5.5 g). This was purified by flash column chromatography using 10% ether in hexane to give pure 9*Z*-aldehyde **17** as an oil (4.2 g, 75% yield): UV λ_{max} 303 (ε = 9288); IR (neat) 1669 (C═O), 1607 (C═C) cm^{-1}; MS *m*/*z* 227.48 (MH^+); ^{1}H NMR (300 MHz, $CDCl_3$) δ 9.63 (d, *J* = 8.2 Hz, 1H), 7.50−7.45 (m, 1H), 7.15−7.10 (m, 2H), 6.52 (s, 1H), 6.01 (dt, *J* = 1.1 and 8.2 Hz, 1H), 2.73 (t, *J* = 6.4 Hz, 2H), 2.46 (m, 2H), 2.43 (s, 3H), 2.09 (s 3H), 1.94−1.86 (m, 2H); ^{13}C NMR (75 MHz, $CDCl_3$) δ 193.37, 159.54, 143.22, 137.01, 136.58, 135.15, 130.15, 129.13, 125.91, 122.73, 120.20, 28.06, 27.19, 25.47, 23.86, 19.88.

(2*Z*,4*E*)-4-[6′-Methyl-3′,4′-dihydro-1′(2′*H*)-naphthalen-1′-ylidene]-3-methyl-2-butenal (18). This preparation employed the alcohol **14** (4.50 g, 20.0 mmol) and IBX (22.1 g, 79.0 mmol) suspended in acetone (80 mL). After the workup described earlier and chromatographic purification was obtained the pure 9(*Z*)-aldehyde **18** as an oil (3.03 g, 68.0% yield): UV λ_{max} 307 (ε = 8052); IR (neat) 1674 (C═O), 1609 (C═C) cm^{-1}; MS *m*/*z* 227.59 (MH^+); ^{1}H NMR (400 MHz, $CDCl_3$) δ 9.63 (d, *J* = 8.2 Hz, 1H), 7.54 (d, *J* = 8.1 Hz, 1H), 7.03 (d, *J* = 8.1 Hz, 1H), 6.96 (s, 1H), 6.53 (s, 1H), 6.00 (dt, *J* = 1.1 and 8.2 Hz, 1H), 2.82 (t, *J* = 6.3 Hz, 2H), 2.49 (m, 2H), 2.32 (s, 3H), 2.09 (s 3H), 1.87−1.81 (m, 2H); ^{13}C NMR (100 MHz, $CDCl_3$) δ 195.48, 161.71, 144.00, 140.56, 140.22, 134.00, 132.12, 131.07, 129.31, 126.52, 121.43, 32.19, 30.74, 27.49, 25.93, 23.28.

(2*Z*,4*E*)-4-[7′-Methyl-3′,4′-dihydro-1′(2′*H*)-naphthalen-1′-ylidene]-3-methyl-2-butenal (19). This preparation employed the alcohol **15** (6.16 g, 27.0 mmol) and IBX (30.8 g, 110 mol) suspended in acetone (100 mL). After the workup described earlier and chromatographic purification was obtained the pure 9(*Z*)-aldehyde **19** as an oil (4.4 g, 72% yield): UV λ_{max} 304 (ε = 6830); IR (neat) 1672 (C═O), 1610 (C═C) cm^{-1}; MS *m*/*z* 227.46 (MH^+); ^{1}H NMR (300 MHz, $CDCl_3$) δ 9.64 (d, *J* = 8.2 Hz, 1H), 7.45 (s, 1H), 7.10−6.98 (m, 2H), 6.56 (s, 1H), 6.00 (dt, *J* = 1.1 Hz & 8.2 Hz, 1H), 2.82 (t, *J* = 6.3 Hz, 2H), 2.48 (m, 2H), 2.35 (s, 3H), 2.09 (s 3H), 1.88−1.80 (m, 2H); ^{13}C NMR (75 MHz, $CDCl_3$) δ 193.11, 159.43, 141.90, 135.53, 135.18, 134.35, 129.37, 129.36, 128.97, 124.84, 119.96, 29.65, 28.51, 25.27, 23.89, 21.22.

(2*Z*,4*E*)-4-[8′-Methyl-3′,4′-dihydro-1′(2′*H*)-naphthalen-1′-ylidene]-3-methyl-2-butenal (20). This preparation employed the alcohol **16** (4.50 g, 20.0 mmol) and IBX (22.1 g, 79.0 mmol) suspended in acetone (80 mL). After the workup described earlier and chromatographic purification was obtained the pure 9(*Z*)-aldehyde **20** as an oil (3.57 g, 80% yield): UV λ_{max} 296 (ε = 7665); IR (neat) 1674 (C═O), 1609 (C═C) cm^{-1}; MS *m*/*z* 227.56 (MH^+); ^{1}H NMR (300 MHz, $CDCl_3$) δ 9.82 (d, *J* = 8.2 Hz, 1H), 7.15−7.09 (m, 2H), 7.03−6.95 (m, 1H), 6.15 (s, 1H), 6.03 (dt, *J* = 1.0 and 8.0 Hz, 1H), 2.65 (t, *J* = 6.5 Hz, 2H), 2.48 (s, 3H), 2.51−2.42 (m, 2H), 2.06 (s 3H), 1.84−1.75 (m, 2H); ^{13}C NMR (75 MHz, $CDCl_3$) δ 193.14, 159.25, 141.58, 140.52, 137.43, 134.47, 129.53, 129.30, 127.35, 126.45, 125.54, 29.97, 28.00, 25.38, 22.93, 21.59.

(2*E*,4*E*,6*Z*,8*E*)-Ethyl 8-[5′-Methyl-3′,4′-dihydro-1′(2′*H*)-naphthalen-1′-ylidene]-3,7-dimethyl-2,4,6-octatrienoate (21). To a flame-dried, three-neck 250 mL round-bottomed flask fitted with a nitrogen inlet, addition funnel, and rubber septum was added NaH (60% suspension in mineral oil, 0.850 g, 21.0 mmol). Dry THF (15 mL, distilled over Na/benzophenone) was added to the flask followed by a solution of triethyl phosphonosenecioate (5.60 g, 21.0 mmol) in dry THF (15 mL). The resulting solution was stirred for 15 min, and then freshly distilled HMPA (5 mL) was added under a nitrogen atmosphere. The flask was covered with aluminum foil and stirred for 15 min. A solution of aldehyde **17** (4.00 g, 18.0 mmol) in dry THF (20 mL) was added dropwise through the addition funnel, and the mixture was then stirred at room temperature for 2.5 h. The reaction mixture was quenched with water (25 mL) and extracted with ether (2 × 75 mL). The combined ether layers were washed with brine (60 mL), dried over Na_2SO_4, and concentrated under vacuum to provide the crude product as an oil. The product was purified by column chromatography (*n*-hexane/ether, 9/1) to give 4.46 g of **21** as a 85:15 mixture of (9*Z*)/(9*Z*,13*Z*) (78% combined yield). Separation of these isomers was achieved by column chromatography using *n*-hexane/benzene (1:1) to obtain pure (9*Z*)-**21** (3.57 g, 60.0% yield) as a yellow oil: UV λ_{max} 334.6 (ε = 28 387); IR (neat) 1706 (C═O), 1610 (C═C) cm^{-1}; MS *m*/*z* 337.71 (MH^+); ^{1}H NMR (300 MHz, $CDCl_3$) δ 7.54−7.48 (m, 1H), 7.15−7.04 (m, 2H), 6.64 (dd, *J* = 4.3 Hz & 11.0 Hz, 1H), 6.42 (s, 1H), 6.22 (d, *J* = 15.5 Hz, 1H), 6.11 (d, *J* = 11.0 Hz, 1H), 5.74 (s, 1H), 4.15 (q, *J* = 7.1 Hz, 2H), 2.72 (t, *J* = 6.4 Hz, 2H), 2.40−2.32 (m, 2H), 2.25 (s, 3H), 2.21 (s 3H), 1.97 (s, 3H), 1.87 (m, 2H), 1.27 (t, *J* = 7.1 Hz, 3H); ^{13}C NMR (75 MHz, $CDCl_3$) δ 167.39, 153.17, 140.79, 139.33, 136.85, 136.25, 134.12, 133.18, 129.40, 128.53, 127.48, 125.81, 122.78, 122.59, 118.52, 59.80, 28.25, 27.36, 24.97, 24.00, 19.97, 14.56, 14.07.

(2*E*,4*E*,6*Z*,8*E*)-Ethyl 8-[6′-Methyl-3′,4′-dihydro-1′(2′*H*)-naphthalen-1′-ylidene]-3,7-dimethyl-2,4,6-octatrienoate (22). This preparation employed a suspension of NaH (60% suspension in mineral oil, 0.479 g, 12.0 mmol) in anhydrous THF (15 mL), a solution of phosphonate ester (3.17 g, 12.0 mol) in anhydrous THF (10 mL), HMPA (4 mL), and a solution of aldehyde **18** (2.26 g, 10.0 mmol) in anhydrous THF (15 mL). After the workup described earlier and chromatographic purification was obtained the ester (2.42 g, 72.0% yield (9*Z* + 9*Z*,13*Z*)) as an oil. Separation of these isomers was achieved by column chromatography using *n*-hexane/benzene (1:1) to obtain pure (9*Z*)-**22** (1.95 g, 58.0% yield): UV λ_{max} 334 (ε = 21 112); IR (neat) 1706 (C═O), 1610 (C═C) cm^{-1}; MS *m*/*z* 337.81 (MH^+); ^{1}H NMR (400 MHz, $CDCl_3$) δ 7.56 (d, *J* = 8.2 Hz, 1H), 7.01 (d, *J* = 8.1 Hz, 1H), 6.92 (s, 1H), 6.64 (dd, *J* = 4.2 and 11.1 Hz, 1H), 6.43 (s, 1H), 6.22 (d, *J* = 15.3 Hz, 1H), 6.10 (d, *J* = 11.0 Hz, 1H), 5.74 (s, 1H), 4.15 (q, *J* = 7.1 Hz, 2H), 2.81 (t, *J* = 6.3 Hz, 2H), 2.40−2.37 (m, 2H), 2.32 (s, 3H), 2.22 (s 3H), 1.97 (s, 3H), 1.84−1.78 (m, 2H), 1.28 (t, *J* = 7.1 Hz, 3H); ^{13}C NMR (100 MHz, $CDCl_3$) δ 167.34, 153.16, 140.80, 138.05, 137.78, 137.57, 134.03, 133.18, 133.04, 129.95, 127.46, 127.16, 124.50, 121.69, 118.46, 59.76, 30.39, 28.85, 24.90, 23.99, 21.22, 14.52, 14.02.

(2*E*,4*E*,6*Z*,8*E*)-Ethyl 8-[7′-Methyl-3′,4′-dihydro-1′(2′*H*)-naphthalen-1′-ylidene]-3,7-dimethyl-2,4,6-octatrienoate (23). This preparation employed a suspension of NaH (60% suspension in mineral oil, 0.878 mg, 22.0 mmol) in anhydrous THF (15 mL), a solution of phosphonate ester (5.81 g, 22.0 mol) in anhydrous THF

dx.doi.org/10.1021/jm5004792 | *J. Med. Chem.* 2014, 57, 5370−5380

(15 mL), HMPA (5 mL), and a solution of aldehyde **19** (4.07 g, 18.0 mmol) in anhydrous THF (20 mL). After the workup described earlier and chromatographic purification was obtained the ester (4.23 g, 70.0% yield (9*Z* + 9*Z*,13*Z*)) as an oil. Separation of these isomers was achieved by column chromatography using *n*-hexane/benzene (1:1) to obtain pure (9*Z*)-**23** (3.69 g, 61.0% yield): UV λ_{max} 333 (ε = 25 568); IR (neat) 1705 (C═O), 1601 (C═C) cm^{-1}; MS *m*/*z* 337.67 (MH^+); ^1H NMR (300 MHz, $CDCl_3$) δ 7.47 (s, 1H), 7.02 (s, 2H), 6.63 (dd, *J* = 4.3 Hz & 11.0 Hz, 1H), 6.45 (s, 1H), 6.23 (d, *J* = 15.3 Hz, 1H), 6.11 (d, *J* = 11.0 Hz, 1H), 5.75 (s, 1H), 4.15 (q, *J* = 7.1 Hz, 2H), 2.81 (t, *J* = 6.3 Hz, 2H), 2.40−2.32 (m, 2H), 2.35 (s, 3H), 2.22 (s 3H), 1.97 (s, 3H), 1.84−1.77 (m, 2H), 1.29 (t, *J* = 7.1 Hz, 3H); ^{13}C NMR (75 MHz, $CDCl_3$) δ 167.25, 153.05, 140.64, 138.24, 135.53, 135.48, 134.90, 134.11, 133.08, 129.29, 128.64, 127.48, 124.96, 122.39, 118.50, 59.70, 29.97, 28.76, 24.82, 24.08, 21.36, 14.49, 14.00.

(2*E*,4*E*,6*Z*,8*E*)-Ethyl 8-[8′-Methyl-3′,4′-dihydro-1′(2′*H*)-naphthalen-1′-ylidene]-3,7-dimethyl-2,4,6-octatrienoate (24). This preparation employed a suspension of NaH (60% suspension in mineral oil, 0.560 g, 14.0 mmol) in anhydrous THF (15 mL), a solution of phosphonate ester (3.70 g, 14.0 mmol) in anhydrous THF (10 mL), HMPA (4 mL), and a solution of aldehyde **20** (2.71 g, 12.0 mmol) in anhydrous THF (15 mL). After the workup described earlier and chromatographic purification was obtained the ester (3.14 g, 78.0% yield (9*Z* + 9*Z*,13*Z*)) as an oil. Separation of these isomers was achieved by column chromatography using *n*-hexane/benzene (1:1) to obtain pure (9*Z*)-**24** (2.58 g, 62.0% yield): UV λ_{max} 328 (ε = 27 316); IR (neat) 1708 (C═O), 1603 (C═C) cm^{-1}; MS *m*/*z* 337.84 (MH^+); ^1H NMR (400 MHz, $CDCl_3$) δ 7.20−7.06 (m, 2H), 6.92 (s, 1H), 6.78 (dd, *J* = 4.3 and 11.1 Hz, 1H), 6.22 (d, *J* = 15.4 Hz, 1H), 6.12 (d, *J* = 11.2 Hz, 1H), 6.05 (s, 1H), 5.76 (s,1H), 4.16 (q, *J* = 7.1 Hz, 2H), 2.63 (t, *J* = 6.5 Hz, 2H), 2.50 (s, 3H), 2.40−2.30 (m, 2H), 2.24 (s 3H), 1.96 (s, 3H), 1.80−1.73 (m, 2H), 1.28 (t, *J* = 7.1 Hz, 3H); ^{13}C NMR (75 MHz, $CDCl_3$) δ 167.36, 153.00, 140.63, 138.52, 137.55, 134.53, 134.08, 133.17, 129.42, 128.71, 127.10, 126.71, 125.32, 118.69, 59.83, 30.21, 27.92, 24.73, 22.96, 21.74, 14.56, 13.92.

(2*E*,4*E*,6*Z*,8*E*)-8-[5′-Methyl-3′,4′-dihydro-1′(2′*H*)-naphthalen-1′-ylidene]-3,7-dimethyl-2,4,6-octatrienoic Acid (1). The 9*Z*-ester **21** (3.02 g, 9.00 mmol) was suspended in methanol (100 mL) and warmed to about 70 °C in an oil bath. An aqueous solution of 2.0 N KOH (45 mL, 90.0 mmol) (prepared with distilled and degassed water) was added to the above suspension and stirred under reflux for 1.5 h. Then the reaction mixture was cooled in an ice bath, diluted with ice-cold water (50 mL), and acidified to pH 1−2 with ice-cold 2 N HCl. The resulting precipitate was filtered, redissolved in ether (100 mL), washed with H_2O (2 × 40 mL), brine (40 mL), dried over Na_2SO_4, and concentrated under vacuum to furnish the final acid **1** (2.64 g, 96.0% yield) as a yellow solid, which was crystallized from ether/*n*-hexanes (1:1) to furnish pure (9*Z*)-**1** (2.05 g, 74.0% yield): mp 189−191 °C [ether/hexanes (1:1)]; UV λ_{max} 324.6 (ε = 28 747); IR (KBr) 2936 (−OH), 1669 (C═O), 1592 (C═C) cm^{-1}; MS *m*/*z* 309.57 (MH^+); ^1H NMR (300 MHz, $CDCl_3$) δ 11.2 (brs, 1H), 7.55−7.45 (m, 1H), 7.15−7.05 (m, 2H), 6.68 (dd, *J* = 4.3 and 11.1 Hz, 1H), 6.42 (s, 1H), 6.29 (d, *J* = 9.7 Hz, 1H), 6.12 (d, *J* = 11.1 Hz, 1H), 5.76 (s, 1H), 2.72 (t, *J* = 6.4 Hz, 2H), 2.40−2.32 (m, 2H), 2.25 (s, 3H), 2.21 (s 3H), 1.98 (s, 3H), 1.92−1.82 (m, 2H); ^{13}C NMR (75 MHz, $CDCl_3$) δ 172.73, 155.78, 141.64, 139.52, 136.88, 136.30, 136.22, 134.13, 133.93, 129.46, 127.44, 125.83, 122.80, 122.55, 117.71, 28.27, 27.36, 25.03, 24.00, 19.98, 14.26.

(2*E*,4*E*,6*Z*,8*E*)-8-[6′-Methyl-3′,4′-dihydro-1′(2′*H*)-naphthalen-1′-ylidene]-3,7-dimethyl-2,4,6-octatrienoic Acid (2). This preparation utilized 9*Z*-ester **22** (1.80 g, 5.40 mmol) suspended in methanol (70 mL) and a solution of 2 N KOH (27 mL, 54.0 mmol) in water (27 mL). After the workup described earlier was obtained the acid **2** (1.58 g, 96.0% yield) as a yellow solid, which was crystallized from ether/*n*-hexane to furnish pure (9*Z*)-**2** (1.16 g, 70.0% yield): mp 173−174 °C [ether/hexanes (1:1)]; UV λ_{max} 326 (ε = 30 749); IR (KBr) 2935 (−OH), 1677 (C═O), 1594 (C═C) cm^{-1}; MS *m*/*z* 309.70 (MH^+); ^1H NMR (400 MHz, $CDCl_3$) δ 11.77 (brs, 1H), 7.56 (d, *J* = 8.0 Hz, 1H), 7.20 (d, *J* = 8.00 Hz, 1H), 6.95 (s, 1H), 6.68 (dd, *J* = 3.8 Hz & 11.2 Hz, 1H), 6.43 (s, 1H), 6.25 (d, *J* = 15.3 Hz, 1H), 6.11 (d, *J* = 11.0 Hz, 1H), 5.76 (s, 1H), 2.81 (t, *J* = 6.1 Hz, 2H), 2.40−2.35 (m, 2H), 2.32 (s, 3H), 2.16 (s 3H), 1.98 (s, 3H), 1.84−1.78 (m, 2H); ^{13}C NMR (100 MHz, $CDCl_3$) δ 172.93, 155.82, 141.69, 138.27, 137.87, 137.69, 134.17, 133.87, 133.04, 130.01, 127.43, 127.20, 124.56, 121.70, 117.73, 30.41, 28.89, 24.99, 24.03, 21.27, 14.25.

(2*E*,4*E*,6*Z*,8*E*)-8-[7′-Methyl-3′,4′-dihydro-1′(2′*H*)-naphthalen-1′-ylidene]-3,7-dimethyl-2,4,6-octatrienoic Acid (3). This preparation utilized 9*Z*-ester **23** (3.00 g, 9.00 mmol) suspended in methanol (100 mL) and a solution of 2 N KOH (45 mL, 90.0 mmol) in water (45 mL). After the workup described earlier was obtained the acid **3** (2.63 g, 95.0% yield) as a yellow solid, which was crystallized from ether/*n*-hexane to furnish pure (9*Z*)-**3** (1.91 g, 69.0% yield): mp 179−181 °C [ether/hexanes (1:1)]; UV λ_{max} 323 (ε = 31 955); IR (KBr) 2930 (−OH), 1679 (C═O), 1592 (C═C) cm^{-1}; MS *m*/*z* 309.71 (MH^+); ^1H NMR (300 MHz, $CDCl_3$) δ 7.47 (s, 1H), 7.02 (s, 2H), 6.68 (dd, *J* = 4.3 and 11.0 Hz, 1H), 6.46 (s, 1H), 6.26 (d, *J* = 15.4 Hz, 1H), 6.12 (d, *J* = 11.0 Hz, 1H), 5.77 (s, 1H), 2.81 (t, *J* = 6.3 Hz, 2H), 2.40−2.35 (m, 2H), 2.35 (s, 3H), 2.23 (s 3H), 1.98 (s, 3H), 1.85−1.77 (m, 2H); ^{13}C NMR (75 MHz, $CDCl_3$) δ 172.74, 155.78, 141.62, 138.49, 135.62, 135.59, 135.05, 134.13, 133.97, 129.39, 128.76, 127.46, 125.06, 122.45, 117.74, 30.03, 28.83, 24.96, 24.15, 21.44, 14.28.

(2*E*,4*E*,6*Z*,8*E*)-8-[8′-Methyl-3′,4′-dihydro-1′(2′*H*)-naphthalen-1′-ylidene]-3,7-dimethyl-2,4,6-octatrienoic Acid (4). This preparation utilized 9*Z*-ester **24** (2.02 g, 6.0 mmol) suspended in methanol (75 mL) and a solution of 2 N KOH (30 mL, 60.0 mmol) in water (30 mL). After the workup described earlier was obtained the acid **4** (1.79 g, 97.0% yield) as a yellow solid, which was crystallized from ether/*n*-hexane to furnish pure (9*Z*)-**4** (1.40 g, 76.0% yield): mp 180−182 °C [ether/hexanes (1:1)]; UV λ_{max} 316.67 (ε = 26 077); IR (KBr) 2949 (−OH), 1675 (C═O), 1593 (C═C) cm^{-1}; MS *m*/*z* 309.7 (MH^+); ^1H NMR (400 MHz, $CDCl_3$) δ 7.20−7.05 (m, 2H), 6.98 (d, *J* = 6.5 Hz, 1H), 6.82 (dd, *J* = 4.3 and 11.0 Hz, 1H), 6.28 (d, *J* = 15.4 Hz, 1H), 6.13 (d, *J* = 10.8 Hz, 1H), 6.05 (s, 1H), 5.78 (s, 1H), 2.63 (t, *J* = 6.4 Hz, 2H), 2.50 (s, 3H), 2.40−2.35 (m, 2H), 2.24 (s 3H), 1.97 (s, 3H), 1.80−1.73 (m, 2H); ^{13}C NMR (75 MHz, $CDCl_3$) δ 172.44, 155.64, 141.47, 140.66, 138.48, 137.76, 134.55, 134.11, 133.89, 129.44, 128.66, 127.67, 126.76, 125.35, 117.79, 30.21, 27.96, 24.79, 22.98, 21.75, 14.12.

4.2. Binding Affinity, Transient Transfection, and Luciferase Reporter Assays. The binding affinity of **1**−**4** to hRXRα-LBD homodimer was measured using a fluorescence quenching method.[22] hRXRα-LBD homodimers (0.5 μM) were excited at 280 nm, and the protein fluorescence was measured at 337 nm with a Cary Eclipse fluorescence spectrophotometer (Varian, Palo Alto, CA). The binding association constant K_a was calculated by using a nonlinear least-squares regression to fit the raw data.[22]

Transient transfection and luciferase reporter assays were performed using a previously reported protocol.[16] At 24 h prior to transfection, human embryonic kidney (HEK) 293 cells were plated at 2 × 10^5 cells per well in six-well plates. Transfection mixtures included 0.2 μg of the Gal4 reporter plasmid pGL4.31[luc2P/Gal4UAS/Hygro] (Promega), 0.5 μg of pCMXGal4-hRARα or pCMX-Gal4-hRXRα expression vector, and 0.01 μg of Renilla luciferase reporter plasmid, pRL-TK. TransIT-LT1 transfection reagent (Mirus) was used. At 24 h after transfection, rexinoid was added to the culture medium. At 48 h after transfection, reporter activity was determined using the dual-luciferase reporter assay (Promega). The EC_{50} of the luciferase assay was determined using a dose response model with two duplicates at four different concentrations (1, 10, 100, 1000 nM).

4.3. Inhibition of Oncogenic Transformation Assay. BOSC23 ecotropic packaging cells at 80−90% confluence were transfected with 30 μg of KLF4-ER, ErB2 or pBpuro (control) plasmid DNA. Virus was collected and filtered at 24 and 48 h after transfection and frozen in liquid nitrogen. Following viral titer, RK3E cells with 30% confluence were infected with virus in the presence of 10 μg/mL Polybrene. After a 15 h infection, virus was removed and RK3E was supplemented with DMEM. Cells infected with KLF4-ER were given DMEM supplemented with DMSO (control), 9cRA, 9cUAB30, **1**, **2**, **3**, and **4** every other day in duplicate at three different concentrations. Three

dx.doi.org/10.1021/jm5004792 | J. Med. Chem. 2014, 57, 5370−5380

weeks after infection, transformed foci were fixed, stained, counted, and analyzed against DMSO control.

4.4. In Vivo Triglyceride Levels, Antiproliferative, and Apoptosis Assays. All animal studies were performed in accordance with the University of Alabama at Birmingham guidelines as defined by the Institutional Animal Care and Use Committee (IACUC-121008309). The TG, antiproliferative, and apoptosis assays were conducted on female Sprague−Dawley rats bearing small mammary cancers. Mammary cancers were induced in 50 day-old female Sprague−Dawley rats by iv injection of the chemical carcinogen *N*-methylnitrosourea (75 mg/kg BW). The animals were fed a Teklad diet according to previous reports.[6] The retinoids tested were mixed into the diet according to the protocols reported previously and fed for 7 days.[6] For the evaluation of the compounds on serum triglycerides, blood was collected from the inferior vena cava at the time of sacrifice of the animals. The blood was kept at 5 °C during centrifugation (3800 rpm for 15 min). Serum was immediately collected and frozen at −85 °C until analyzed for triglycerides.[23] The infinity triglycerides assay kit was purchased from Thermo DMA. For evaluation of antiproliferative index, animals were injected with bromodeoxyuridine (BRDU) 2 h prior to killing using CO_2. Cancers were removed and fixed with 10% formalin. Cell proliferation and cell apoptosis were performed as previously reported.[6] The proliferation/apoptotic indices were calculated as the ratio of proliferation/apoptosis of treated animals to vehicle fed animals.

4.5. Protein Purification, Crystallization, and X-ray Crystallography. The hRXRα-LBD (T_{223}-T_{462}) was overexpressed in *Escherichia coli* and purified using AKTA purifier system.[7] The hRXRα-LBD homodimers were isolated from a gel filtration chromatography. The protein was mixed with a 4-fold excess of UAB rexinoids and then 5-fold excess of GRIP-1 coactivator peptide. The ternary complexes were crystallized using vapor diffusion technique in hanging drops.[7] Diffraction data of crystals were collected at synchrotron source of Advanced Proton Source (APS) at Argonne National Laboratory or on a Rigaku IV+ diffractometer at UAB. The collected diffraction data were processed using the program D*Trek.[24] The structures were solved using the molecular replacement method with a high-resolution hRXRα-LBD structure with its ligand deleted as a search model (PDB code 3OAP). The structures were refined using CNS software.[25] A complete summary of data for these structures is given in the Supporting Information. Interactions between ligand/peptide and hRXRα-LBD were analyzed using a program Ligand-Protein Contacts (LPC)/Contacts of Structural Units (CSU).[26] All structures were prepared using PyMol (*The PyMOL Molecular Graphics System*, version 0.99; Schrödinger, LLC: New York).

■ ASSOCIATED CONTENT

Ⓢ Supporting Information

Tables containing the crystallographic data collection, refinement statistics, and elemental analysis data. This material is available free of charge via the Internet at http://pubs.acs.org.

■ AUTHOR INFORMATION

Corresponding Authors

*W.J.B.: phone, 1-205-934-8288; e-mail, wbrou@uab.edu.

*D.D.M.: phone, 1-205-934-8285; fax, 1 205 934-2543; e-mail, muccio@uab.edu.

Notes

The authors declare no competing financial interest.

■ ACKNOWLEDGMENTS

We thank Dr. Ellen Li (Washington University in St. Louis, MO) for providing the protein expression vector. We appreciate critical reading and helpful comments provided by Dr. Matthew B. Renfrow. This work was supported by grants from the National Institutes of Health (NIH) Grant 2 P50 CA089019 (D.D.M.) and the Komen Foundation (Grant BCTR 20000690) (D.D.M.).

■ ABBREVIATIONS USED

RXR, retinoid X receptor; RAR, retinoic acid receptor; RA, retinoic acid; LBD, ligand binding domain; IBX, *o*-iodoxybenzoic acid; RKE, rat kidney epithelial; SCC, squamous cell carcinoma; TG, triglyceride; GRIP, 1-glucocorticoid receptor interacting peptidie 1; LBP, ligand binding pocket; THF, tetrahydrofuran; HMPA, hexamethylphosphoramide; TLC, thin layer chromatography; BRDU, bromodeoxyuridine

■ REFERENCES

(1) Boehm, M. F.; Zhang, L.; Badea, B. A.; White, S. K.; Mais, D. E.; Berger, E.; Suto, C. M.; Goldman, M. E.; Heyman, R. A. Synthesis and structure−activity relationships of novel retinoid X receptor-selective retinoids. *J. Med. Chem.* **1994**, *37*, 2930−2941.

(2) Duvic, M.; Martin, A. G.; Kim, Y.; Olsen, E.; Wood, G. S.; Crowley, C. A.; Yocum, R. C. Phase 2 and 3 clinical trial of oral bexarotene (Targretin capsules) for the treatment of refractory or persistent early-stage cutaneous T-cell lymphoma. *Arch. Dermatol.* **2001**, *137*, 581−593.

(3) Miller, V. A.; Benedetti, F. M.; Rigas, J. R.; Verret, A. L.; Pfister, D. G.; Straus, D.; Kris, M. G.; Crisp, M.; Heyman, R.; Loewen, G. R.; Truglia, J. A.; Warrell, R. P., Jr. Initial clinical trial of a selective retinoid X receptor ligand, LGD1069. *J. Clin. Oncol.* **1997**, *15*, 790−795.

(4) Atigadda, V. R.; Vines, K. K.; Grubbs, C. J.; Hill, D. L.; Beenken, S. L.; Bland, K. I.; Brouillette, W. J.; Muccio, D. D. Conformationally defined retinoic acid analogues. 5. Large-scale synthesis and mammary cancer chemopreventive activity for (2*E*,4*E*,6*Z*,8*E*)-8-(3′,4′-dihydro-1′(2′*H*)-naphthalen-1′-ylidene)-3,7-dimethyl-2,4,6-octatrienoic acid (9cUAB30). *J. Med. Chem.* **2003**, *46*, 3766−3769.

(5) Muccio, D. D.; Brouillette, W. J.; Breitman, T. R.; Taimi, M.; Emanuel, P. D.; Zhang, X.; Chen, G.; Sani, B. P.; Venepally, P.; Reddy, L.; Alam, M.; Simpson-Herren, L.; Hill, D. L. Conformationally defined retinoic acid analogues. 4. Potential new agents for acute promyelocytic and juvenile myelomonocytic leukemias. *J. Med. Chem.* **1998**, *41*, 1679−1687.

(6) Grubbs, C. J.; Lubet, R. A.; Atigadda, V. R.; Christov, K.; Deshpande, A. M.; Tirmal, V.; Xia, G.; Bland, K. I.; Eto, I.; Brouillette, W. J.; Muccio, D. D. Efficacy of new retinoids in the prevention of mammary cancers and correlations with short-term biomarkers. *Carcinogenesis* **2006**, *27*, 1232−1239.

(7) Xia, G.; Boerma, L. J.; Cox, B. D.; Qiu, C.; Kang, S.; Smith, C. D.; Renfrow, M. B.; Muccio, D. D. Structure, energetics, and dynamics of binding coactivator peptide to the human retinoid X receptor alpha ligand binding domain complex with 9-cis-retinoic acid. *Biochemistry* **2011**, *50*, 93−105.

(8) Boerma, L. J.; Xia, G.; Qui, C.; Cox, B. D.; Chalmers, M. J.; Smith, C. D.; Lobo-Ruppert, S.; Griffin, P. R.; Muccio, D. D.; Renfrow, M. B. Defining the communication between agonist and coactivator binding in the retinoid X receptor alpha ligand binding domain. *J. Biol. Chem.* **2014**, *289*, 814−826.

(9) Desphande, A.; Xia, G.; Boerma, L. J.; Vines, K. K.; Atigadda, V. R.; Lobo-Ruppert, S.; Grubbs, C. J.; Moeinpour, F. L.; Smith, C. D.; Christov, K.; Brouillette, W. J.; Muccio, D. D. Methyl-substituted conformationally constrained rexinoid agonists for the retinoid X receptors demonstrate improved efficacy for cancer therapy and prevention. *Bioorg. Med. Chem.* **2014**, *22*, 178−185.

(10) Vedell, P. T.; Lu, Y.; Grubbs, C. J.; Yin, Y.; Jiang, H.; Bland, K. I.; Muccio, D. D.; Cvetkovic, D.; You, M.; Lubet, R. Effects on gene expression in rat liver after administration of RXR agonists: UAB30, 4-methyl-UAB30, and Targretin (bexarotene). *Mol. Pharmacol.* **2013**, *83*, 698−708.

(11) Kawamura, M.; Cui, D. M.; Hayashi, T.; Shimada, S. Lewis acid-catalyzed Friedel−Crafts acylation reaction using carboxylic acids as acylating agents. *Tetrahedron Lett.* **2003**, *44*, 7715−7717.

(12) Zhang, X.; De Los Angeles, J. E.; He, M. Y.; Dalton, J. T.; Shams, G.; Lei, L.; Patil, P. N.; Feller, D. R.; Miller, D. D.; Hsu, F. L. Medetomidine analogs as alpha 2-adrenergic ligands. 3. Synthesis and biological evaluation of a new series of medetomidine analogs and their potential binding interactions with alpha 2-adrenoceptors involving a "methyl pocCket". *J. Med. Chem.* **1997**, *40*, 3014−3024.
(13) Romanov-Michailidis, F.; Guenee, L.; Alexakis, A. Enantioselective organocatalytic iodination-initiated Wagner−Meerwein rearrangement. *Org. Lett.* **2013**, *15*, 5890−5893.
(14) Allegretto, E. A.; McClurg, M. R.; Lazarchik, S. B.; Clemm, D. L.; Kerner, S. A.; Elgort, M. G.; Boehm, M. F.; White, S. K.; Pike, J. W.; Heyman, R. A. Transactivation properties of retinoic acid and retinoid X receptors in mammalian cells and yeast. Correlation with hormone binding and effects of metabolism. *J. Biol. Chem.* **1993**, *268*, 26625−26633.
(15) Bourguet, W.; Ruff, M.; Chambon, P.; Gronemeyer, H.; Moras, D. Crystal structure of the ligand-binding domain of the human nuclear receptor RXR-alpha. *Nature* **1995**, *375*, 377−382.
(16) Jiang, W.; Deng, W.; Bailey, S. K.; Nail, C. D.; Frost, A. R.; Brouillette, W. J.; Muccio, D. D.; Grubbs, C. J.; Ruppert, J. M.; Lobo-Ruppert, S. M. Prevention of KLF4-mediated tumor initiation and malignant transformation by UAB30 rexinoid. *Cancer Biol. Ther.* **2009**, *8*, 289−98.
(17) Lindeblad, M.; Kapetanovic, I. M.; Kabirov, K. K.; Dinger, N.; Mankovskaya, I.; Morrisey, R.; Martin-Jimenez, T.; Lyubimov, A. Assessment of oral toxicity and safety of 9-cis-UAB30, a potential chemopreventive agent, in rat and dog studies. *Drug Chem. Toxicol.* **2011**, *34*, 300−10.
(18) Kolesar, J. M.; Hoel, R.; Pomplun, M.; Havighurst, T.; Stublaski, J.; Wollmer, B.; Krontiras, H.; Brouillette, W.; Muccio, D.; Kim, K.; Grubbs, C. J.; Bailey, H. E. A pilot, first-in-human, pharmacokinetic study of 9cUAB30 in healthy volunteers. *Cancer Prev. Res.* **2010**, *3*, 1565−1570.
(19) Leung, C. S.; Leung, S. S.; Tirado-Rives, J.; Jorgensen, W. L. Methyl effects on protein−ligand binding. *J. Med. Chem.* **2012**, *55*, 4489−4500.
(20) Herz, W. Azulenes. VII. A novel rearrangement in the synthesis of azulenes. *J. Am. Chem. Soc.* **1956**, *78*, 1485−1494.
(21) Gedye, R. N.; Westaway, K. C.; Arora, P.; Bisson, R.; Khalil, A. H. The stereochemistry of the Wittig reactions of allylic phosphoranes and phosphonate esters with aldehydes. *Can. J. Chem.* **1977**, *55*, 1218−1228.
(22) Cheng, L.; Norris, A. W.; Tate, B. F.; Rosenberger, M.; Grippo, J. F.; Li, E. Characterization of the ligand-binding domain of human retinoid-X receptor-alpha expressed in *Escherichia-coli*. *J. Biol. Chem.* **1994**, *269*, 18662−18667.
(23) McGowan, M. W.; Artiss, J. D.; Strandbergh, D. R.; Zak, B. A peroxidase-coupled method for the colorimetric determination of serum triglycerides. *Clin. Chem.* **1983**, *29*, 538−542.
(24) Otwinowski, Z.; Minor, W. Processing of X-ray diffraction data collected in oscillation mode. *Macromol. Crystallogr., Part A* **1997**, *276*, 307−326.
(25) Brunger, A. T.; Adams, P. D.; Clore, G. M.; DeLano, W. L.; Gros, P.; Grosse-Kunstleve, R. W.; Jiang, J. S.; Kuszewski, J.; Nilges, M.; Pannu, N. S.; Read, R. J.; Rice, L. M.; Simonson, T.; Warren, G. L. Crystallography & NMR system: a new software suite for macromolecular structure determination. *Acta Crystallogr., Sect. D: Biol. Crystallogr.* **1998**, *54*, 905−921.
(26) Sobolev, V.; Sorokine, A.; Prilusky, J.; Abola, E. E.; Edelman, M. Automated analysis of interatomic contacts in proteins. *Bioinformatics* **1999**, *15*, 327−32.